ELSEVIER

Polymer 42 (2001) 6043–6055

polymer

www.elsevier.nl/locate/polymer

Effects of superimposing rotational components on monoaxial die-drawing of polymers in their solid state

S.M. Mannell, L. Mascia*

Institute of Polymer Technology and Materials Engineering, Loughborough University of Technology, Loughborough, Leicestershire LE11 3TU, UK

Received 14 August 2000; received in revised form 15 January 2001; accepted 29 January 2001

Abstract

Solid state processing is a very efficient method of introducing molecular orientation in polymeric products. In this respect, die-drawing of polymers has received considerable attention as it allows to achieve very high draw ratios in comparison to free-axial drawing.

In this work, square billets were drawn through dies made up of four axially symmetrical sections to form convergent channels with spiralling walls. The materials studied were high density polyethylene (HDPE) and quenched (amorphous) polyethylene terephthalate (PET) to produce filamentary products with draw ratios up to 9:1.

The results have shown that the rotational components of the deformations resulting from the spiralling walls, which are superimposed onto axial extensions, alter the balance between tensile and shear stresses acting on the material in passing through the die. This has considerable effect on the drawing forces and properties of the final products. Noteworthy is the relative amount of free-axial drawing in the longitudinal direction, and associated elastic recovery, which cause substantial differences in the overall draw ratio imposed on to the filaments. This effect is particularly pronounced for PET. At the same time the spiralling walls of dies reduce the overall level of orientation in the amorphous phase and brings about an increased resistance to splitting under transverse compression and a reduction in shrinkage at higher temperatures.

Keywords: Die drawing; High density polyethylene; Polyethylene terephthalate

1. Introduction

Solid state processing of continuous products, conventionally carried out by extrusion or die-drawing, has attracted considerable attention in scientific research for its ability to introduce high levels of molecular orientation in the final products [1–3]. Although the majority of studies have been concerned with processes that develop monoaxial orientation in the axial direction, some variants to these have been reported for the introduction of biaxial orientation in continuous products with rectangular or annular cross-sections [4,5]. Mascia and Zhao have used converging–diverging dies, designed on the principle of pure shear deformations, to produce flat extrudates with a biaxial orientation bias in the transverse direction [6–8].

Another interesting development in solid state processing to produce biaxial orientation is the superimposition of rotational deformations on axial stretching. Zachariades achieved biaxial orientation by using a die geometry capable of imposing curvilinear deformation on the material through a combination of compressive and rotational forces [9]. Mascia et al. have illustrated this principle by means of a conventional biaxial stretcher where the gripping line of the clamps was offset from the two perpendicular drawing axes. In these studies they were also able to demonstrate some of the advantages of drawing polymers with superimposed distortion components over conventional axial drawing, notable among these is the higher dimensional stability of the resulting products [10].

Most studies reported on solid state extrusion or die drawing are related to the production of filamentary products exhibiting monoaxial orientation. More recently it has been shown that higher draw ratios are obtained in die-drawing processes by adding an elongational axial component to shear deformations in the die. According to Shaw this results from the reduction in the velocity gradient across the axial direction, which alters the balance of forces in favour of the elongational components [11]. Coates and Ward [12], on the other hand, have attributed the achievement of higher production rates in the combined extrusion die-drawing process to the ability of the polymer to deform at an optimal strain rate which allows it to neck away from the die walls before it reaches the die exit.

* Corresponding author. Tel.: +1509-223339; fax: +1509-223949.
E-mail address: l.mascia@lboro.ac.uk (L. Mascia).

0032-3861/01/$ - see front matter
PII: S0032-3861(01)00095-7

Irrespective of the manner in which monoaxial orientation is brought about the resulting filamentary products suffer from a low torsional rigidity and a high propensity to splitting along the longitudinal direction.

The present study was initiated with the view to determine whether a control of the morphology can be achieved by imposing deformations in the hoop direction while the material is drawn axially through converging dies. This situation is analogous to that reported in earlier studies on biaxial orientation [10] and is to be achieved by drawing a polymer feedstock through dies with spiralling walls which impose rotational deformations on the polymer simultaneously to axial elongations.

In any case the superimposition of rotational components on axial stretching provides a different deformation history to conventional die drawing and is expected to alter the orientation state of the polymer in the final product.

2. Theoretical interpretations

2.1. Rotational shear

Rotational shear can be imposed on an element of a material through rotation of adjacent cross-sections. In order to realise a twisting deformation it is necessary to have the means to grip the material so that rotational forces can be applied to different cross-sections. For this reason square sections have been used in the analysis and for the experimental verification.

The helical geometry of the die wall prevents warping of the cross-section so that at any point along the length of the die the only shear in the transverse direction is the rotational shear strain. This makes the torsion analysis of a square section bar equivalent to that of a circular rod [13]. In the spiralling wall dies of this study the rotational shear is applied about the axis of the square section billet so that the magnitude of the rotational shear strain, γ_φ will depend on the angle of twist, θ, over the length, l, and on the radial distance, r, from the axis of rotation.

For relatively small angles of rotations, as in the present case, the rotational shear strain, γ_φ, is

$$\gamma_\varphi = \frac{r\theta}{l}.$$

For a square section element the radial distance from the axis to the surface increases along the wall to a maximum at the corner. This results also in a non-uniform variation of strain through the thickness of the sample.

2.2. Rotational shear and extensional deformation

If a linear extensional deformation is imposed after a rotational shear, its effect will tend to reduce the contribution of rotational shear strain component to the total deformation of a particular element. This can be illustrated by considering the effect of tensile drawing an helically twisted square section, as shown in Fig. 1a. Each element of material increases in length according to the draw ratio. The magnitude of the rotational shear strain, after drawing, $\gamma_{\varphi f}$ is the same as that required to straighten the product. The latter is a recovered shear strain and, therefore, will have a negative value. Fig. 2 shows the rotational shear strain of an element on the surface of a cylinder in the helical product before and after tensile drawing, $\gamma_{\varphi 0}$, and $\gamma_{\varphi f}$, respectively.

Assuming that the shear strain increases linearly from the central axis, for both directions of rotation, it is clear that

$$\gamma_{\varphi 0} = \frac{r_0\theta}{l_0} \tag{1}$$

and

$$\gamma_{\varphi f} = -\frac{r_f\theta}{l_f}.$$

The initial and final lengths of the element, l, and the radial distance, r, from the axis, before and after drawing, can be related to each other via the draw ratio, λ

$$l_f = \lambda l_0 \tag{2}$$

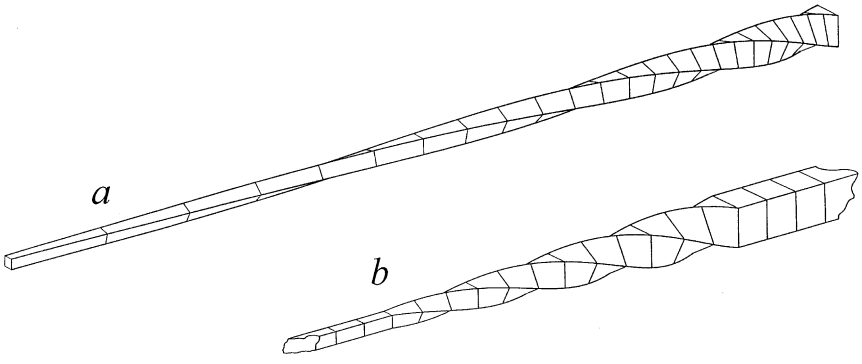

Fig. 1. Extensional and shear strains in square-section spiralling convergent dies. (a) Extension superimposed onto the initial rotational shear strain at the die entry, resulting in an increase in spiral pitch along the length. (b) Extension with constant spiral pitch along the length, represented by equidistant cross-section line contours.

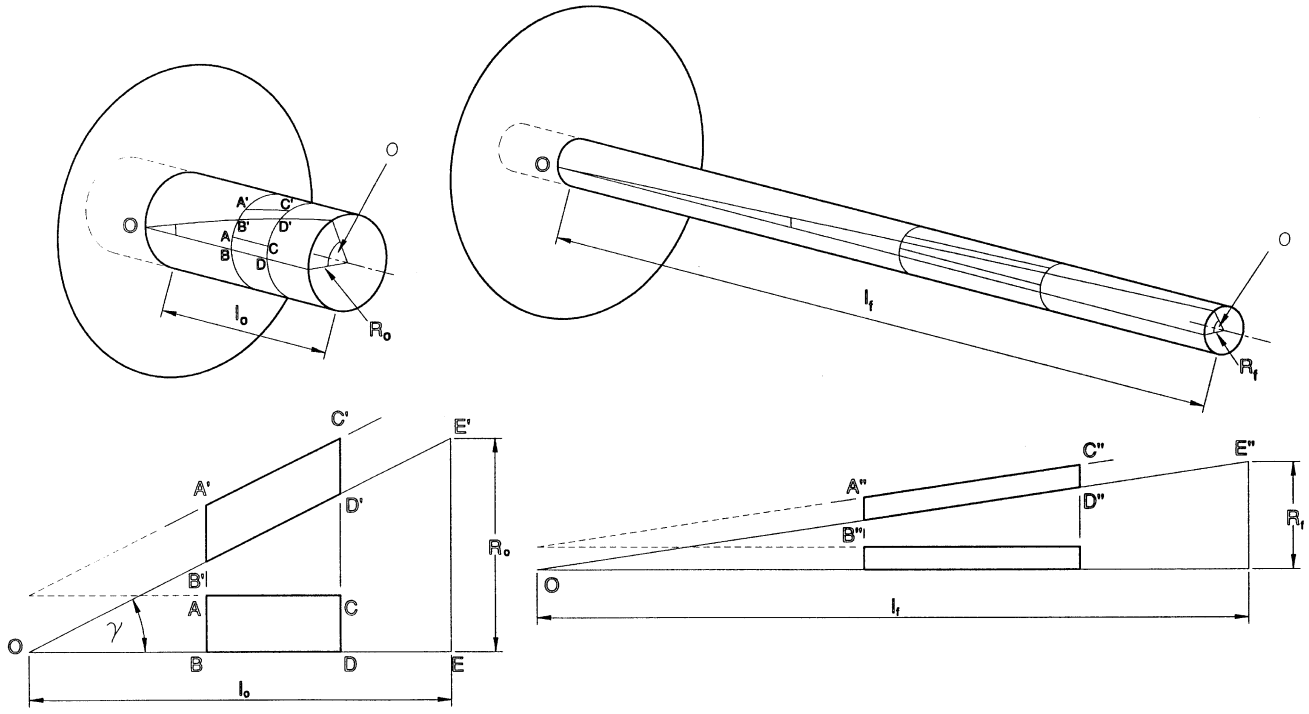

Fig. 2. Principle of rotational shear strain reduction resulting from axial extension.

and

$$r_f = \frac{r_0}{\sqrt{\lambda}}.$$

Therefore, for tensile drawing the amount of rotational shear strain of an element after experiencing an extensional draw ratio λ can be related to its initial rotational shear by the following expression:

$$\gamma_{\varphi f} = -\gamma_{\varphi 0}(\lambda)^{-3/2}. \tag{3}$$

The difference between $\gamma_{\varphi 0}$ and $\gamma_{\varphi f}$ is equal to the shear strain recovered through the axial extension, γ_{tensile}

$$\gamma_{\text{tensile}} = -\gamma_{\varphi 0}\left(1 - \frac{1}{(\lambda)^{3/2}}\right). \tag{4}$$

If a square section convergent die is such that its cross-sections rotate at a constant rate along the central axis, it will form spiralling walls with a constant pitch, as shown in Fig. 1b. Assuming that the material is deformed plastically, and uniformly, in passing through this spiralling wall channel it will emerge at the exit with a helical shape having a pitch equal to that of the die.

The rate of twist along the die axis can be expressed by ω, where $\omega = (\theta/l)$.

The rotational shear strain of an element at any point within the die at distance r from the die axis is given by

$$\gamma_\varphi = \frac{r\theta}{l} = r\omega. \tag{5}$$

At the die entrance a sudden rotational shear is imposed on the material $\gamma_{\varphi(\text{entry})}$, which is given by

$$\gamma_{\varphi\text{entry}} = r_{\text{entry}}\omega. \tag{6}$$

At the die exit the rotational shear strain, $\gamma_{\varphi(\text{exit})}$, imposed on an element, by the counter rotation at the die exit by the gripping actions of the drawing clamps, is given by

$$\gamma_{\varphi\text{exit}} = -r_{\text{exit}}\omega. \tag{7}$$

This is equal to the amount of rotational shear required to straighten the element. Combining the above equations is possible to obtain a relationship for the rotational shear strain recovered at the die exit relative to that applied at the die entrance;

$$\gamma_{\varphi\text{exit}} = -\gamma_{\varphi\text{entry}}(\lambda)^{-1/2}. \tag{8}$$

The amount of reverse shear strain that must applied to a die-drawn product in order to straighten the walls will, therefore, depend on the way the extension has been imposed during drawing. A lower reverse shear strain is required for a tensile drawn helical product, after being subjected to an initial rotational shear strain (Fig. 1a), than for one drawn through a spiralling die with a constant pitch (Fig. 1b). This provides evidence for the existence of an additional rotational shear strain arising from deformation through a constant pitch spiralling die. Although in both processes the shear strain of an element is reduced by extensional deformations, the amount is less when using a die with constant pitch. In effect the latter die will provide some additional rotational shearing as the material passes through it, which compensates for the amount lost through

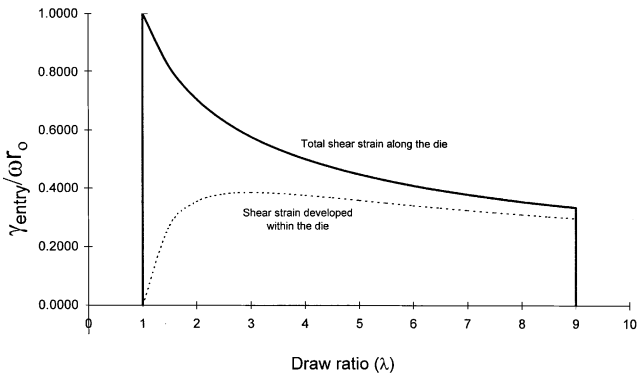

Fig. 3. Rotational shear evolution through a uniaxiallly convergent spiralling die.

axial extension. The magnitude of this progressive rotational shear strain imposed by the spiralling walls if the die can be found from the difference between the reverse shear applied to the die-drawn billet and that of tensile drawn filaments, i.e.

$$\gamma_{die} = \gamma_{\varphi entry}(\lambda)^{\frac{-1}{2}} - \gamma_{\varphi entry}(\lambda)^{-3/2,} \tag{9}$$

$$\gamma_{\varphi die} = \frac{\gamma_{\varphi entry}}{\sqrt{\lambda}}\left(1 - \frac{1}{\lambda}\right). \tag{10}$$

In summary, the three components of rotational shear strain experienced by an element of material passing through a convergent spiralling-walls die with a constant pitch along its axis are

(i) At the entry instantaneous rotational shear strain at the die entry, $\gamma_{\varphi entry} = r_{entry}\omega$.
(ii) Through the die
  (a) rotational shear strain due to linear extension, $\gamma_{\varphi tensile} = -\gamma_{\varphi entry}(1 - (1/(\lambda)^{3/2}))$ (negative because it is a recovered strain);
  (b) progressive rotational shear strain through the die, $\gamma_{\varphi die} = (\gamma_{\varphi entry}/\sqrt{\lambda})((1 - (1/\lambda))$.
(iii) Recovered rotational shear strain at the die exit, $\gamma_{\varphi exit} = -\gamma_{\varphi entry}(\lambda)^{-1/2}$ (equal and opposite to the total shear strain accumulated within the die).

Fig. 3 illustrates how the the rotational shear strain imposed at the die entry changes in passing through the die. The calculations were made for a nominal draw ratio of 9:1 and the curve was normalised with respect to the initial radial distance from the die axis and with respect to the helix angle formed by the edge of the die channel.

It is worth noting that the reverse rotational shear at the die exit cancels the rotational shear from the drawn product, i.e. it is forced to go to zero by applying a shear strain of equal magnitude in the opposite direction. The curve in Fig. 3 indicates that the shear strain at the exit becomes only one third of the value imposed at the die entry when a constant pitch is maintained in the spiralling wall. This is to say also that if the level of shear strain imposed at the die entry is to be maintained the angle of twist would have to increase gradually by a total factor of 3 from the entry to the exit of the die. The purpose of this analysis is to demonstrate this very principle, within the limitations imposed by the non-uniformity of the strain across the thickness, which is expected to be accentuated by the anisotropy that the polymer acquires along the die length through axial orientation. Moreover, the rotational shear strains imposed on the drawn products by the spiralling walls are, therefore, expected to change only the strain history of the materials in passing through the die and not the overall magnitude and type of strains.

3. Experimental

3.1. Dies and drawing assembly

The exact geometry of the channels of the dies used in this study is illustrated in Fig. 4. The dies were built in four sections, so that they could be opened to examine the deformations and state of the polymer during drawing. In Fig. 5 (top) are shown two consecutive quadrants of the die, each providing one wall of the channel, so that when assembled together (bottom section of Fig. 5) they will form a complete spiralling channel. The dies were fixed in a die assembly and mounted on a Hounsfield tensometer which was fitted with an environmental chamber to heat the die and the polymer feedstock to the required temperature (Fig. 6).

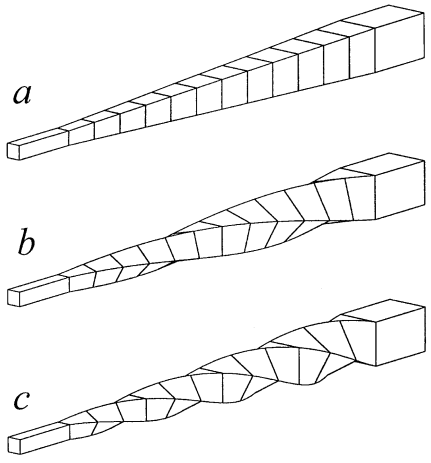

Fig. 4. Geometry of square-section convergent spiralling dies. Channel walls tapering angle with respect to central axis is 2.0°; nominal draw ratio resulting from convergence is 9:1; cross-sections at entry is 6 mm × 6 mm, cross-section at exit is 2 mm × 2 mm: (a) straight die, (b) smaller angle spiralling die (Helical Die A): 1.5°/mm axial length, (c) larger angle spiralling die (Helical Die B):3.0°/mm axial length.

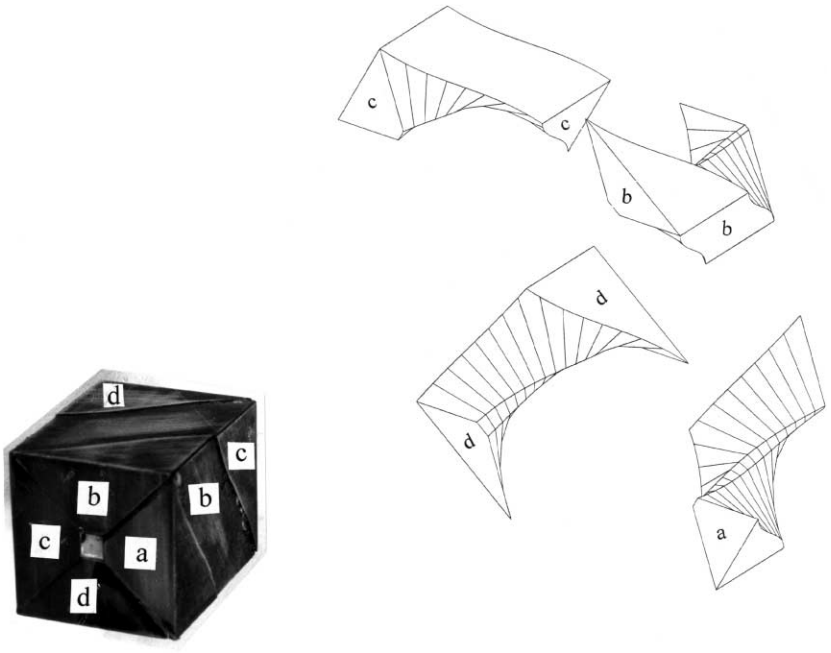

Fig. 5. Spiralling die assembly block showing the four wall sections and spacer block and wall sections of spiralling dies assembly: (a) Helical Die A:90° wall twist (1.5°/mm) (b) Helical Die B:180° wall twist (3.0°/mm).

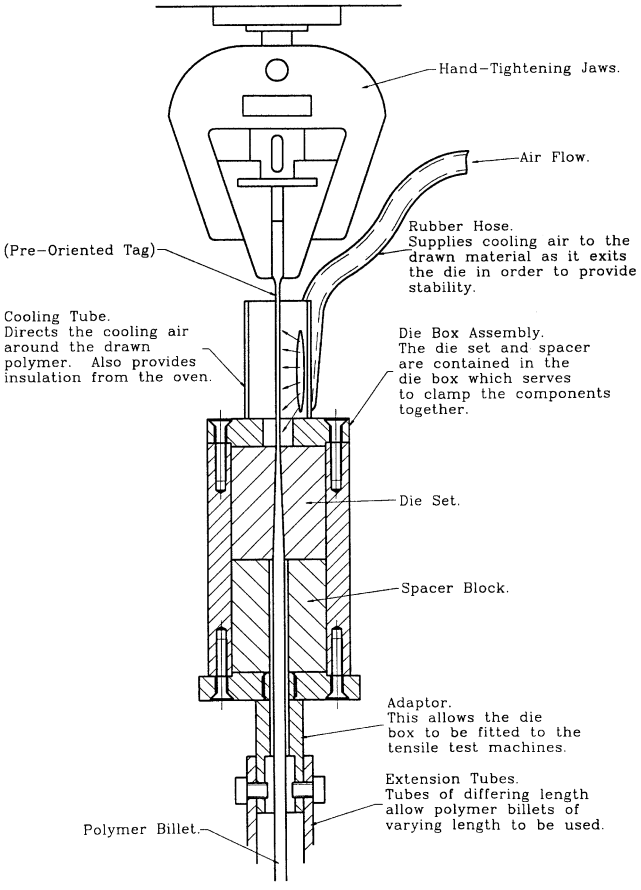

Fig. 6. Die assembly block fitted into environmental cabinet of a Hounsfield tensile testing machine.

3.2. Materials

The feedstock was in the form of square sectioned billets, 6 mm × 6 mm, about 30 cm in length produced from the following materials:

(a) A high molecular weight of linear polyethylene in the form of sheets, 6 mm thick, supplied by Solidur, and designated as type 500. These were machined into square rods to produce the feedstock for the die-drawing experiments.
(b) Polyethylene terephthalate with an intrinsic viscosity value of 1.05, supplied by Eastman Chemical under the trade name of Copolyester 13339. This was extruded into square section rods with quench-cooling to obtain an amorphous structure. The rods were machined to size in order to remove any geometric irregularities.

3.3. Die-drawing studies

The heating chamber of the Hounsfield Tensometer was first calibrated to ensure that temperature variations were not more than 2°C in the zone containing the die assembly. Sections of the feedstock, about 30 cm long, were drawn through the die by the moving upper jaws gripping the pre-drawn tail end of the billet threaded through the die orifice. Both temperature and drawing speed were varied over a wide range for both materials. The drawn filaments were cooled by air as they emerged through the die and removed after being cooled to room temperature under tension while the lower end of the feed stock was still within the die. The dimensions of the drawn filaments were

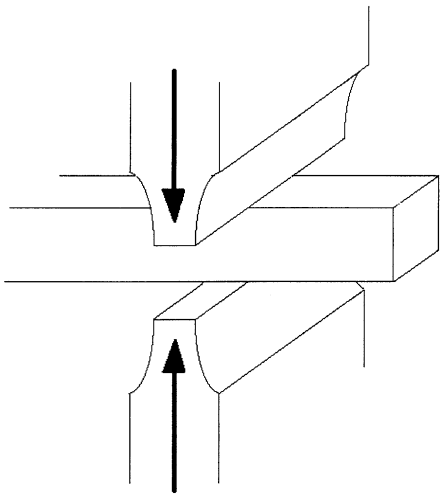

Fig. 7. Plane-strain compression gig for measuring splitting resistance of drawn filaments.

subsequently measured from the die entry region and along the length outside the die so that the actual draw ratio imposed by the die-drawing operation could be calculated for each processing conditions.

In all cases different draw ratios were achieved by starting with billets of different cross-section areas.

3.4. Linear shrinkage

Thermal retraction measurements were carried out on drawn PET samples by immersions in constant temperature baths, respectively water for measurements at 85 and 100°C and oil for tests at 120°C. Experiments carried out in earlier work have shown that there is no difference in shrinkage values when samples were heated in air or in water [14]. Consequently the environment used to induce the shrinkage is not expected to be an influential factor.

3.5. Tensile modulus

Tensile tests were carried out on a JJ Lloyd machine equipped with a laser extensometer to measure the strain in the central regions of the specimens.

The grip distance was set at 110 mm and the cross-head speed at 100 mm/min, giving a straining rate of 0.0015/s. The Young's modulus was calculated from the slope of the linear plot of the load against extension.

3.6. Compression tests

Compression tests were carried out on samples of HMWPE up to failure using a plane-strain compression gig, as shown in Fig. 7. The contact surface of the specimens was coated with a hydrocarbon grease to minimise lateral constraints. These tests were carried out to measure the length of the split formed along the longitudinal direction of the drawn filament as a means of assessing the effect of die geometry on the ductility in the transverse direction. Samples of drawn PET, however, did not produce this type of failure, possible due to the relatively low draw ratios achieved.

3.7. Birefringence measurements

Birefringence measurements were made on various thin

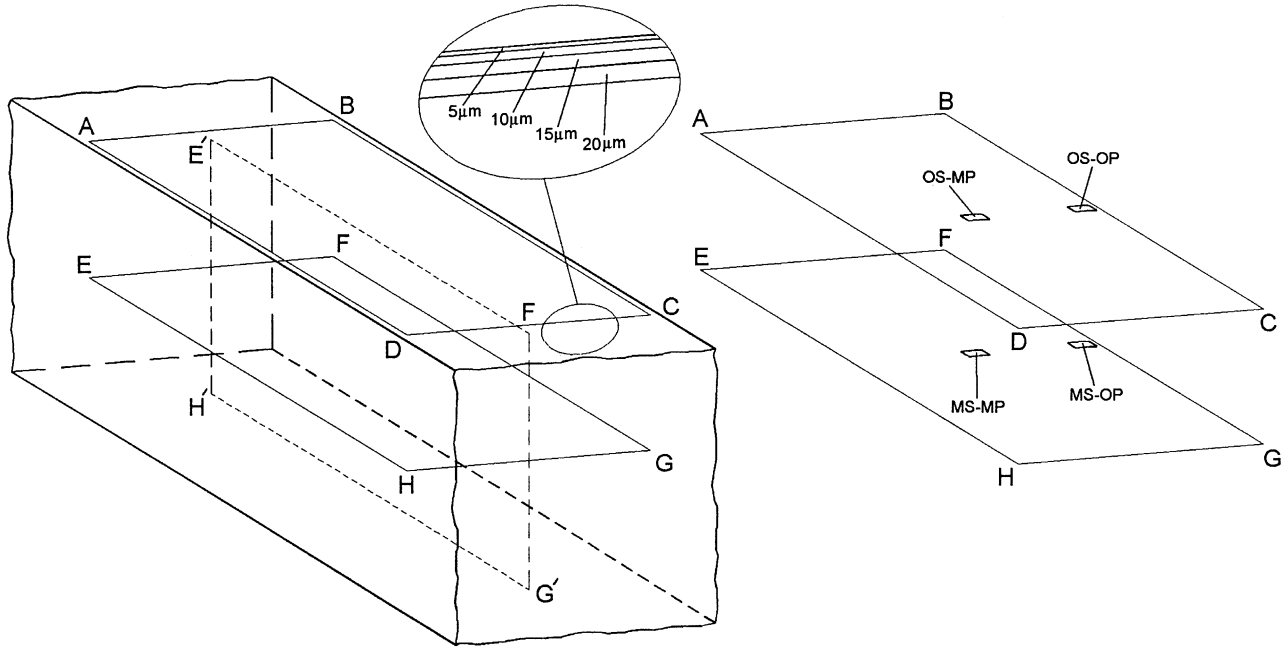

Fig. 8. Sections of drawn filaments showing positions where samples were taken for birifringence measurements. OS-MP = outer layers mid-section; OS-OP = outerlayers edge-section; MS-MP = central region mid-section; MS-OP = central region edge-section.

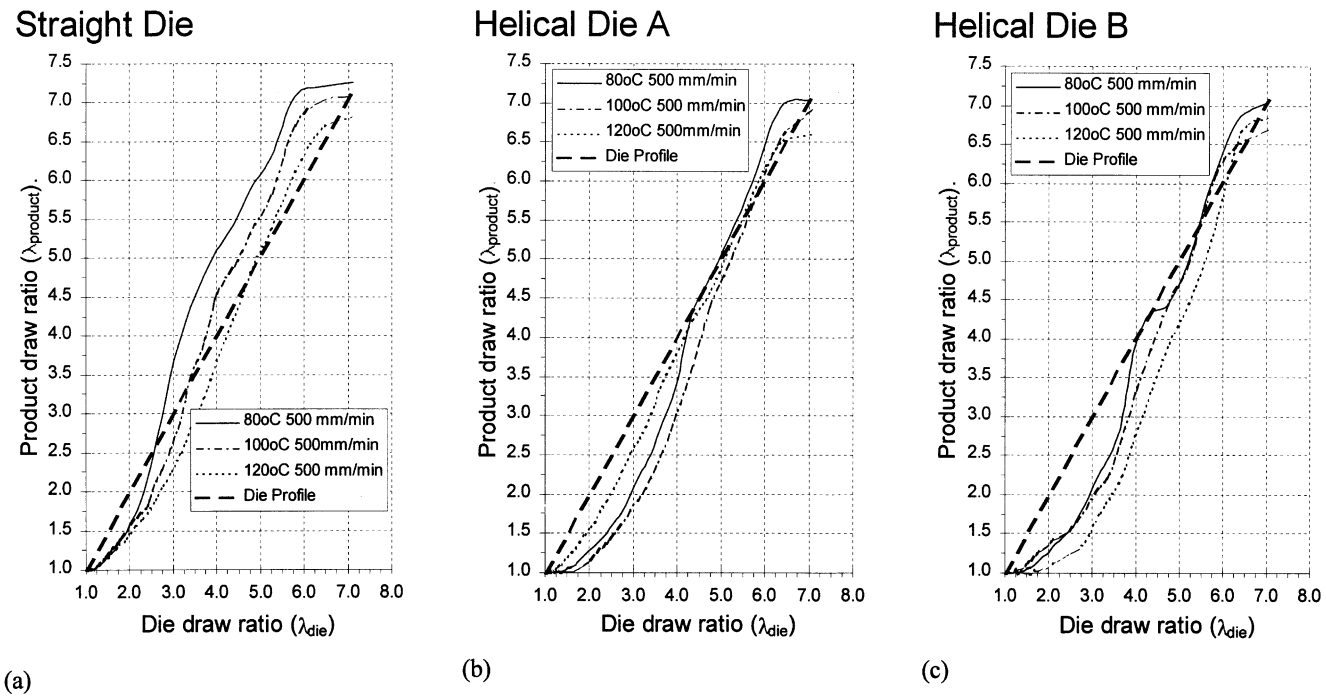

Fig. 9. Product draw ratio as a function of nominal die-draw ratio for HDPE filaments drawn at different temperatures through the straight die and spiralling dies (details in Fig. 4).

sections of drawn products, using a Ehringhaus compensator to obtain the optical path difference (OPD) values. Only HMWPE samples were examined to establish the effects of operation conditions on the variation of orientation through the cross-section of the samples. This is expected to be primarily determined by the geometry of the channels rather than the nature of the material.

The OPD values for each selected region of the samples were measured for various thickness sections, respectively, 5, 10, 15 and 20 μm, and the birefringence was calculated from the slope of the plot of OPD versus thickness, in order to eliminate errors arising from the plastic deformations imposed by the microtoming knife (Fig. 8).

Birefringence measurements were made on sections taken across the thickness of the drawn products in successive steps. The angle formed by the principal axis with the longitudinal edge of each section was also recorded with the aid of the rotating microscope stage in order to determine whether there was any deviation of the axial orientation direction from the longitudinal axis of the die. Thin section samples were also taken in the middle of the wall (sections OS-MP and MS-MP) and towards the edge of the specimen (sections OS-OP and MS-OP) in Fig. 9 (right). As the width of the sample is 3 mm the distance between the points where the readings were taken is only about 1 mm.

3.8. Thermal analysis

Thermal analysis was carried out on both feedstock and drawn samples using a DuPont Instrument 910 DSC apparatus. Measurements were made in a nitrogen atmosphere at a heating rate of 10°C/min for polyethylene and 20°C/min for PET samples. The melting enthalpy was used to calculate the degree of crystallinity using a value of 64.6 cal/g for polyethylene and 32 cal/ g for PET as the reference enthalpy values for the respective pure crystals.

4. Results and discussion

In Fig. 9a–c are shown plots of the actual draw ratio recorded on the drawn filaments against the nominal draw ratio, calculated from the geometry of the channel of the die, for experiments carried out with HMWPE at constant extension rate and at various temperatures.

Similar plots were made for experiments carried out on amorphous PET using the same experimental conditions. These are shown in Fig. 10a–c. Both diagrams clearly reveal a major effect of the transverse rotation imposed by the spiralling walls of the die channel on the discrepancy between nominal draw ratio and the actual values obtained in the drawn filaments.

A comparison of the data in Fig. 9a–c with those in Fig. 10a–c also highlights the substantial difference in behaviour between HMWPE and PET, which can be exemplified by the observation that for the polyolefin samples the spiralling of the walls brings about a gradual decrease in the actual draw ratio imposed on the final product, while the effect is the reverse for the drawing of PET samples.

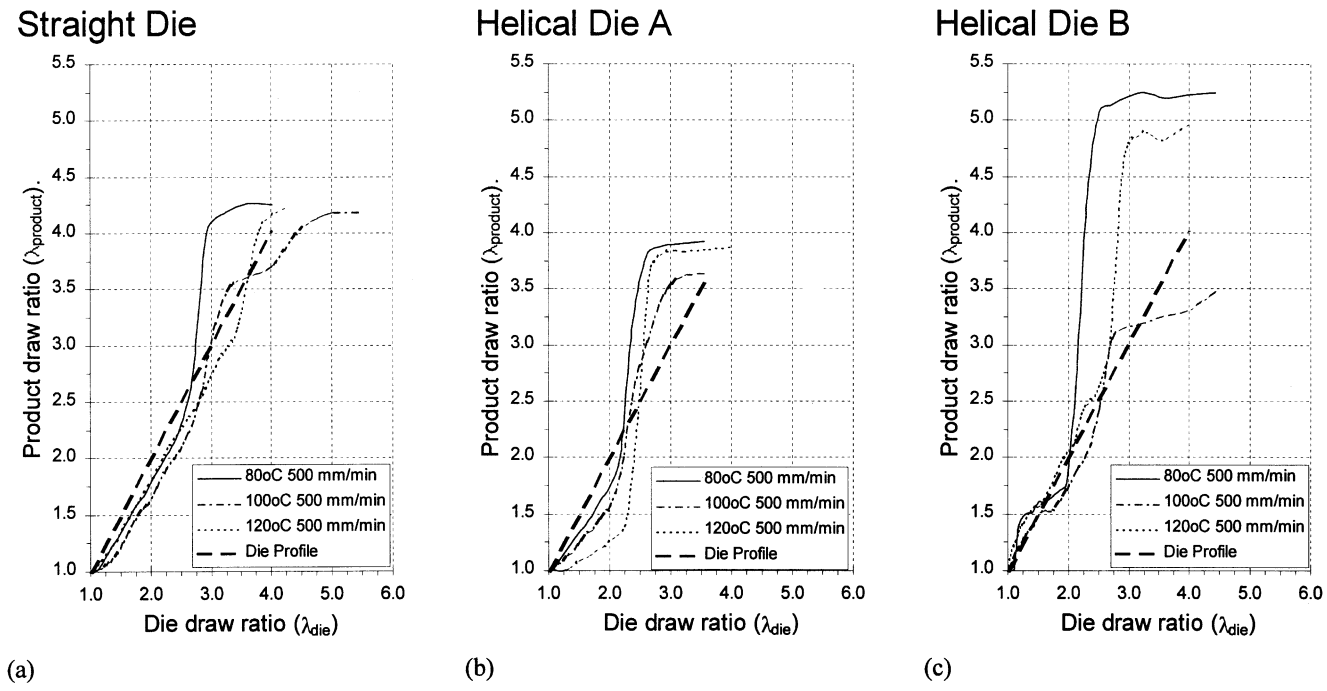

Fig. 10. Product draw ratio as a function of nominal die-draw ratio for PET filaments drawn at different temperatures through the straight die and spiralling dies (details in Fig. 4).

The difference in the behaviour of the two materials at low draw ratios can be attributed to the varying amount of post-die recovery of the axial extension, which is much higher for HMWPE than PET filaments. For the case of HMWPE the recovery of the axial extension is enhanced by the fact that the drawn filaments at the die exit are at a temperature quite near to the thermodynamic melting point. This means that there is a large proportion of polymer chains still in the amorphous (molten) state, which will give rise to considerable shrinkage when the drawing stress is removed.

For the case of HDPE samples at high draw ratios the straight die allows the filaments to be drawn further by the axial forces, while for the spiralling dies tensile extensions are constrained by the spiralling walls, so that the discrepancy between actual and nominal draw ratio values is minimal.

The geometric configuration of the die walls, however, has a much more dramatic effect on the drawing behaviour of PET. The spiral die with the lower helix angle produces filaments whose draw ratio is lower than the values expected from the geometry of the channels. The much larger amount of axial stretching taking place in the spiral dies than the straight die is caused by the fact that yielding takes place nearer to the die entry, owing to the larger magnitude of rotational shear deformations (see Fig. 3). It is interesting to note that in all cases the peak drawing forces registered were always lower for spiralling dies. The larger the helix angle the greater the reduction in drawing forces. This observation is predictable from consideration of yield criteria.

The change in recovery for HMWPE taking place during processing, designated here as 'elastic recovery', at different draw ratios and at various drawing temperatures is shown in Fig. 11. These indicate that there is a progressive increase in elastic recovery with increasing spiralling angle of the die walls, which is associated with the reduced level of axial orientation as a result of the superimposed rotational deformations (see later).

For both materials, however, there appears to be a change in behaviour at some critical draw ratio above which the actual draw ratio becomes higher than the nominal draw ratio (see Figs. 9 and 10). This can also be attributed to the difference in both level of stabilisation of the orientation and extent of elastic recovery taking place after drawing.

It is instructive to note that, for the case of PET, the thermal data plotted in Fig. 12 indicate that there is no distinct difference in the degree of crystallinity between the samples produced with the straight die and those obtained with the helical die, even though a clear trend exists for both dies with respect to the increase in level of crystallinity the drawing temperature is increased. The thermal data on HMWPE were less conclusive.

By analogy to the results from a previous study [10] it can be deduced that the rotational (transverse) deformations reduce the level of orientation within the amorphous phase, while the final degree of crystallinity is determined primarily by the thermal conditions.

An additional discrepancy in behaviour between PET and HMWPE is revealed from a comparison of the data in Figs. 13 and 14 containing plots of the actual draw ratio recorded on the samples against the drawing temperature for different drawing rates. One notes firstly that the drawing

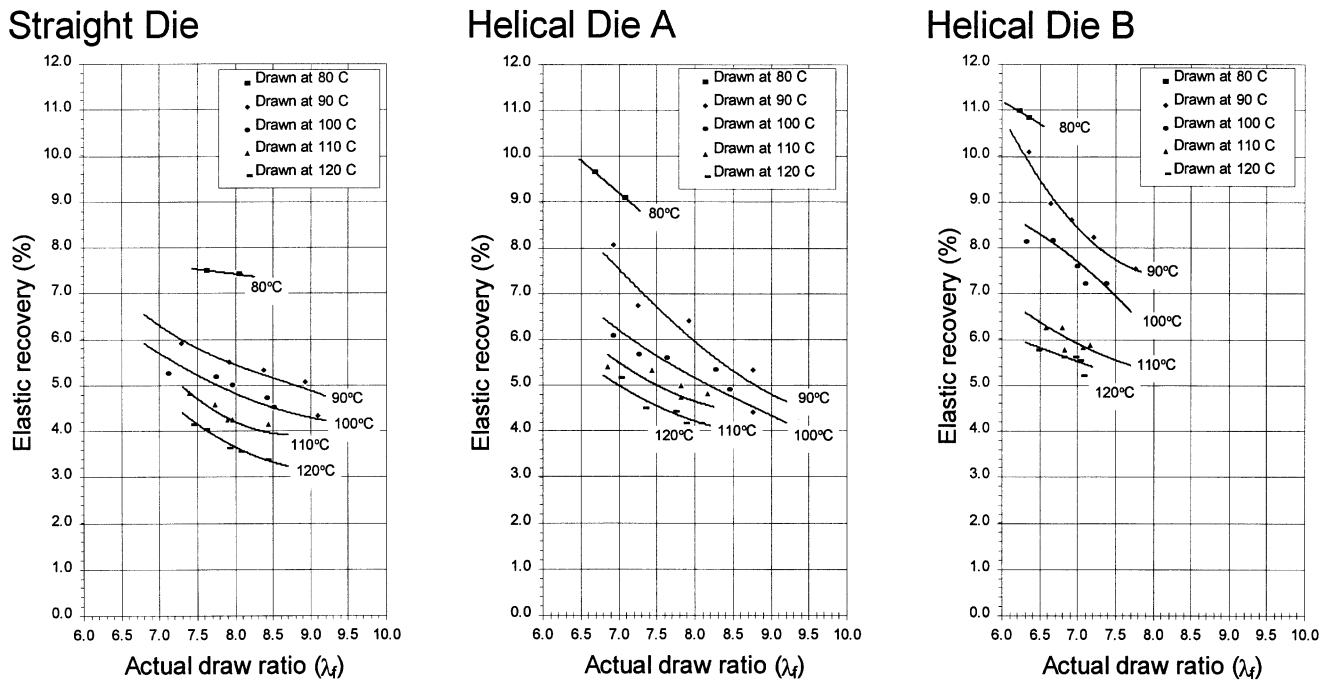

Fig. 11. Elastic recovery, at die exit, for HDPE filaments as a function of product draw ratio for straight and spiralling dies. Experiments carried out at 500 mm/min at different temperatures.

speed has a very large effect on the imposed draw ratio for the case of HMWPE but not so much for PET. Furthermore for the case of HMWPE there is a gradual reduction in the recorded draw ratio with the introduction of spiralling deformations in the die, due to the larger extent of recovery, and that the actual draw ratio tends to decrease with increasing drawing temperature. For PET, on the other hand, a minimum in the actual draw ratio is observed at around 100°C with increasing drawing temperature, which corresponds to the temperature at which one normally observes the highest rate of strain induced crystallisation.

The temperature effect for PET, however, is much more

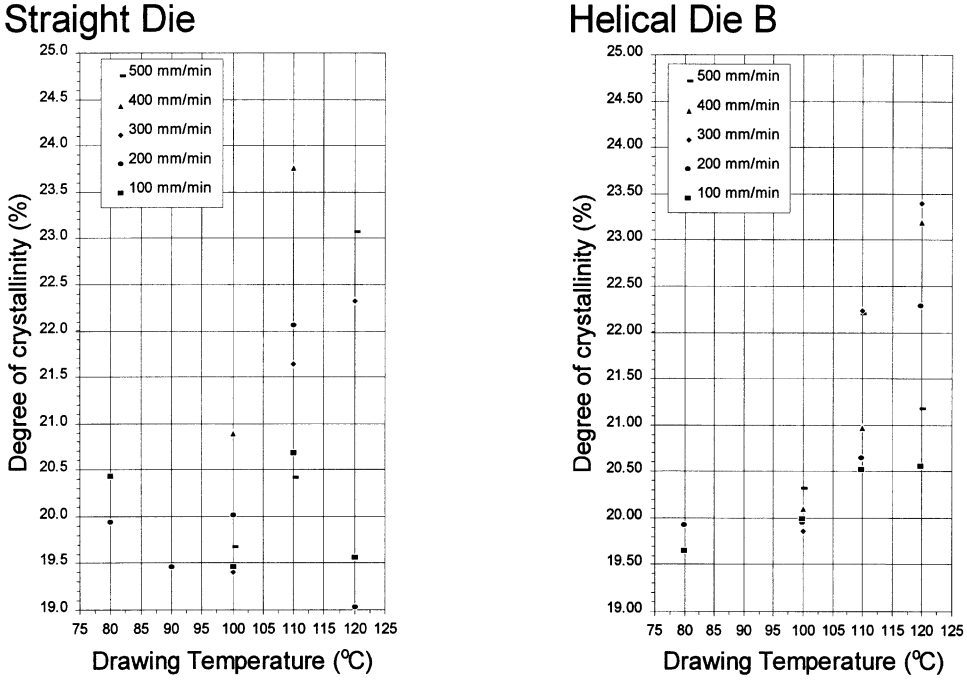

Fig. 12. Degree of crystallinity of HDPE filaments drawn through spiralling dies as function of drawing temperature for experiments carried out at different drawing rates.

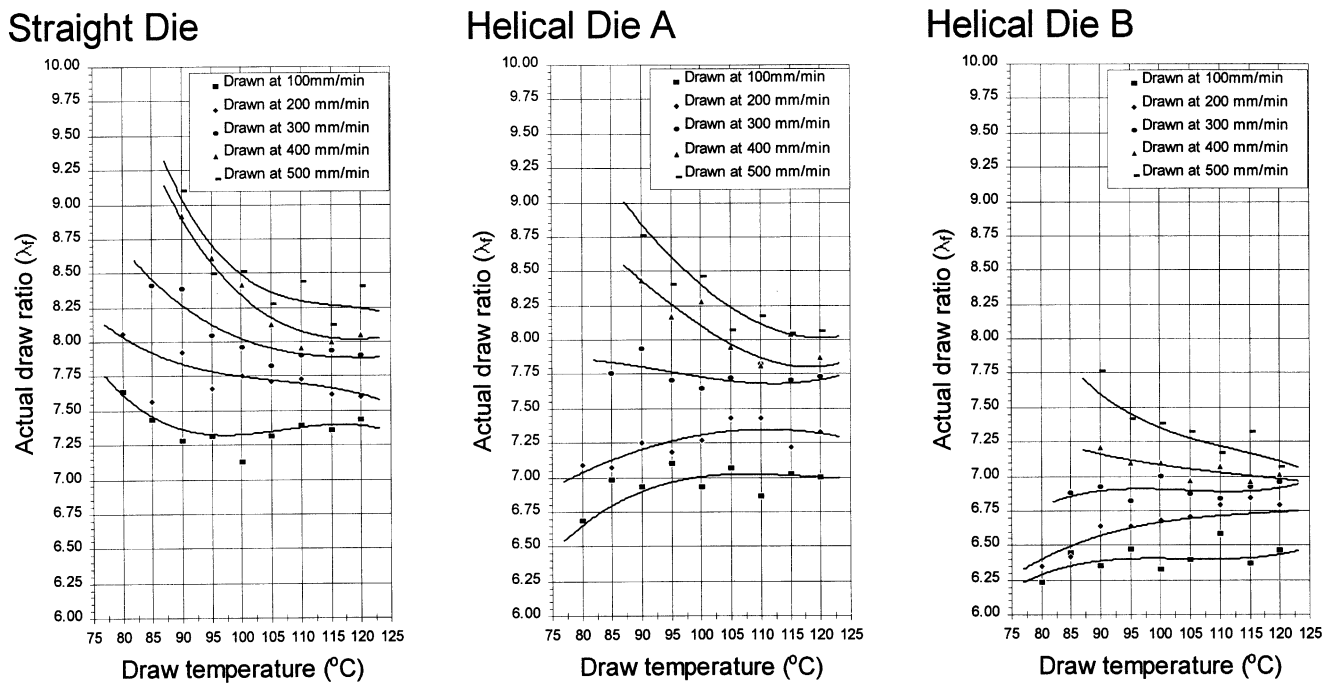

Fig. 13. Actual draw ratio as a function of drawing temperature for HDPE filaments drawn through the straight die and spiralling dies.

pronounced with spiralling dies than for the straight die, which is a reflection of the effects of the difference in stability of the orientation in the sample overall.

In Fig. 15 are reported the changes in birefringence through the cross-section of HMWPE filaments drawn at 100°C for nominal draw ratio of 7:1 These plots show that, while the samples drawn through the straight-wall die display a constant birefringence through the cross-section, for the case of spiral dies the birefringence values are lower in the middle sections and increases from a minimum value along the central axis to a maximum at the wall. The variation in birefringence though the cross-section becomes greater with increasing spiralling angle and the same pattern is repeated at all draw temperatures (Fig. 16). In examining the data in Fig. 15 it is apparent that, while the low birefringence values in the centre of the specimens produced

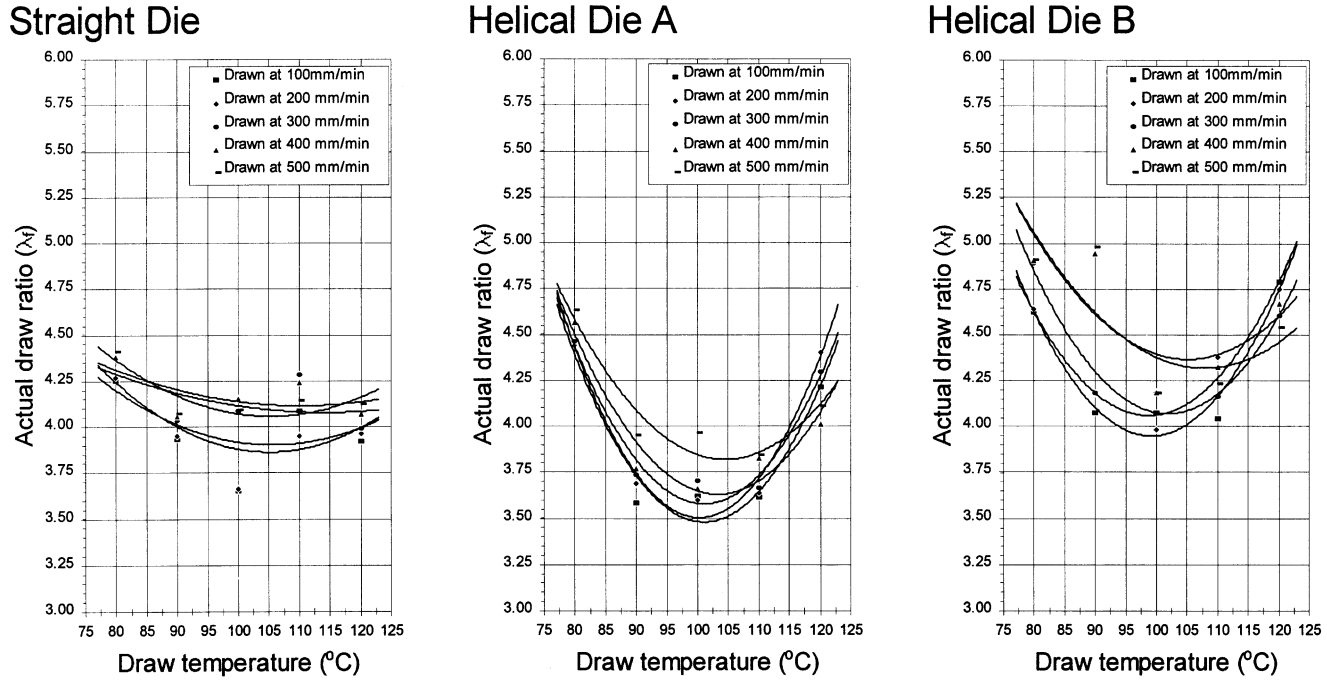

Fig. 14. Actual draw ratio as a function of drawing temperature for PET filaments drawn through the straight die and spiralling dies.

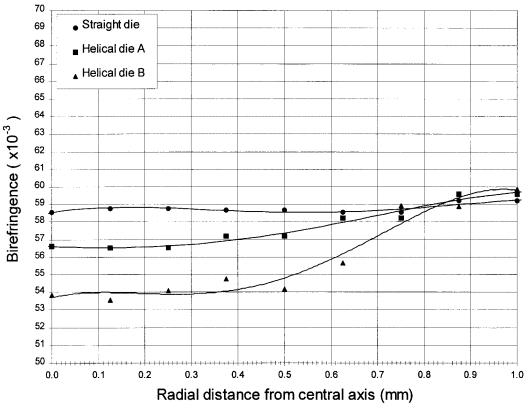

Fig. 15. Birefringence evolution through the cross-section of HDPE filaments drawn through the straight die and spiralling dies.

with the spiralling die are due to the lower true draw ratio, the increase in birefringence near the surface must be associated with the imposed rotational shear strain imposed on the material in passing through the die. The reverse shear imposed on the specimens, after exiting from the die, does not reduce the level of orientation in the surface outer layers because of the constrain imposed in these areas by the gripping forces of the clamps. It is worth noting that no appreciable difference in birefringence was observed between the samples taken at the mid section (OS-MP and MS-MP) and those near the edge (OS-OP and MS-OP) identified in Fig. 3. This indicates that the radial distance difference for the two sections has a negligible effect in the history of the deformation for the final product.

The resemblance of these data to the variation of the angle of principal birefringence with the radial distance from the central axis (Fig. 17) is a possible confirmation for the 'freezing' of the outer surface orientation by the gripping action of the clamps. The discrepancy between the angle of principal birefringence and that formed by the corners of the cross-sections of the die channel is due to

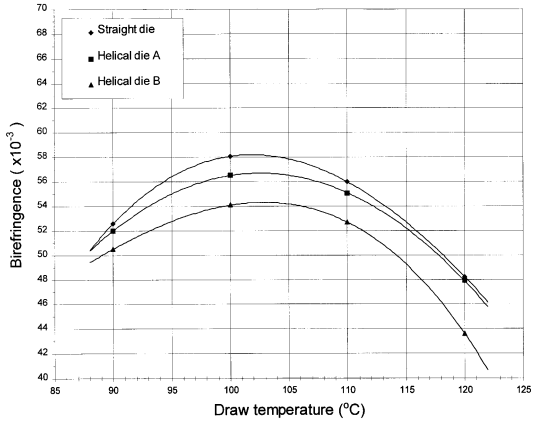

Fig. 16. Mid-section birefringence of HDPE filaments drawn through the straight die and spiralling dies as a function of draw temperature.

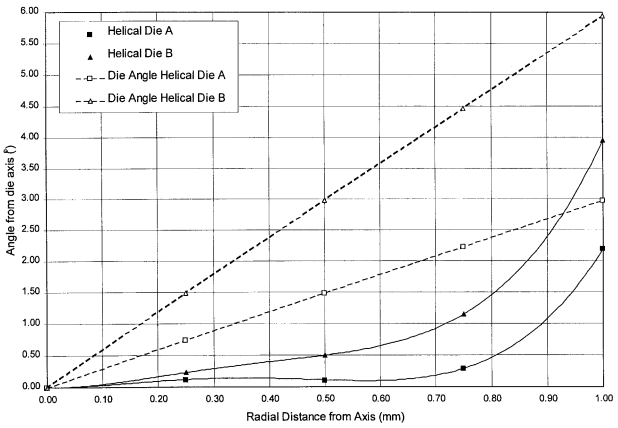

Fig. 17. Variation of angle of principal birefringence axis relative to central die axis through the cross-section of filaments of HDPE drawn through spiralling dies, and comparison with angle formed by each corner of the die cross-section.

the elastic recovery of the rotational shear when the filaments are removed from the clamps.

In Fig. 18 it is shown that the reduction in overall level of orientation in samples drawn with the spiral dies causes a very large reduction in the value of Young's modulus in the axial direction. This is also reflected in a higher ductility of the filaments in the transverse direction, as evidenced by a reduction in the length of the splits formed along the axial direction in the plane compression tests.

Taken in conjunction with the lower thermal shrinkage recorded for filaments produced with spiralling-wall dies (see Fig. 19) it can be deduced that the rotational shear components have the effect of reducing the level of orientation within the amorphous phase. This suggests that the decrease in draw ratio for filaments produced with the spiralling-wall dies at the lower end of draw ratios, is due to the axial shrinkage taking place through molecular relaxations in the amorphous phase. A conclusion, which is borne out also by the elastic recovery data (Fig. 11).

These explanations are consistent with the previous observations by Mascia et al. [10] on the increased dimensional stability of biaxially drawn products, simultaneously subjected to rotational deformations. At the same time these interpretations are supported by the findings of Wilson [15] about the direct correlation between modulus and thermal shrinkage with the orientation in the amorphous phase for PET fibres produced under different tensile drawing conditions. Similarly, Bhatt et al. [16] have associated the high shrinkage forces in PET fibres to the high level of orientation in the amorphous phase.

In this respect it is worth noting that the thermal shrinkage of filaments produced with the convergent straight-wall die is much more sensitive to drawing speed than in

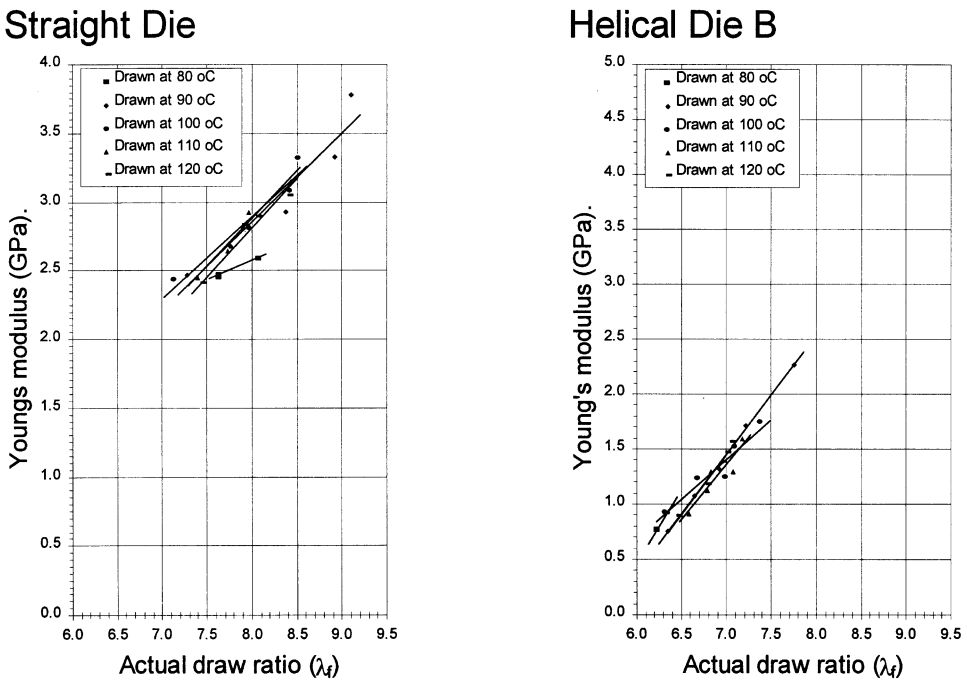

Fig. 18. Young's modulus of PET filaments as a function of actual draw ratio for the straight die and the larger angle spiralling die.

filaments obtained with spiralling dies, even though the thermal shrinkage decreases with increasing drawing speed in all cases.

5. Conclusions

The main conclusions that can be derived from this work is that the rotational deformations imposed by the spiralling walls of convergent dies, in conjunction with the reverse shear imposed after exiting from the die, have an appreciable effect on both processing behaviour and properties of die-drawn products. More specifically:

(a) The magnitude of the drawing forces is reduced proportionally to the helix angle of the spiralling walls.

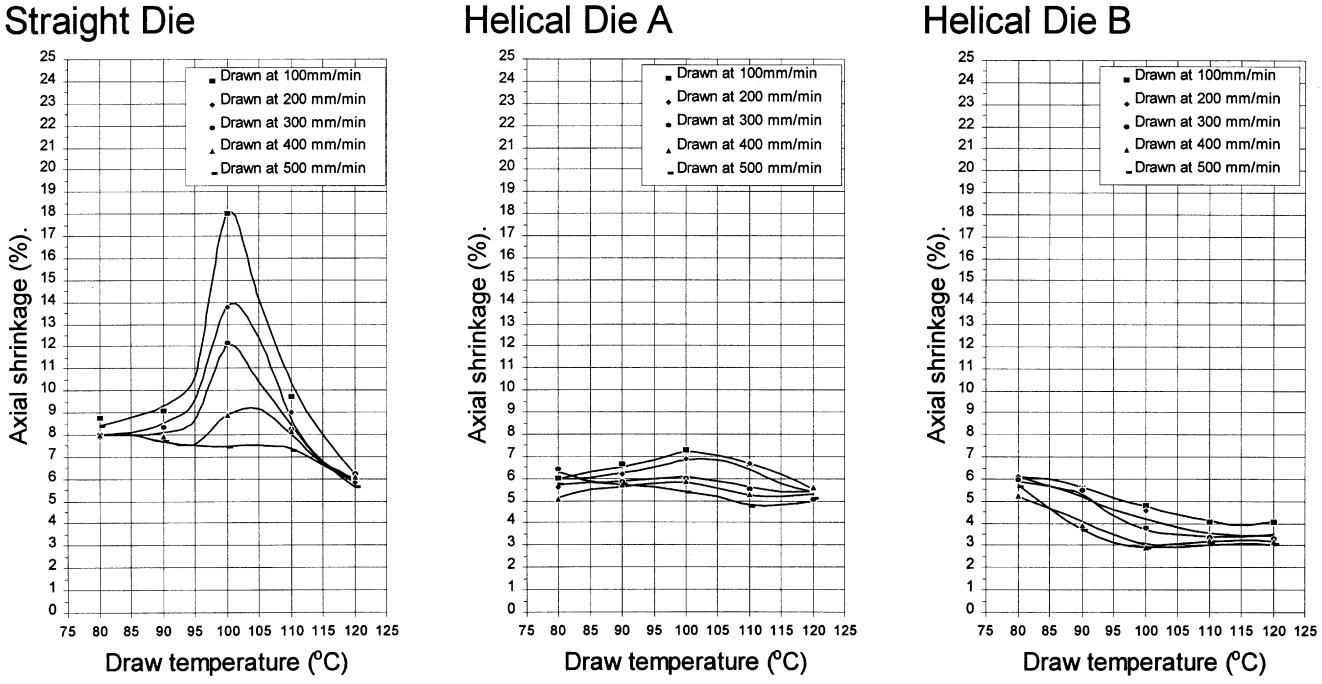

Fig. 19. Axial shrinkage of PET filaments as a function of draw temperature for samples drawn through the straight die and spiralling dies.

This is a consequence of the transverse shear deformations imposed by the spiralling walls in the die entry regions which reduces the level of axial stresses required to bring about yielding of the material. The magnitude of this effect is greater for PET than HDPE irrespective of the processing conditions, such as temperature and drawing speed.

(b) This overall birefringence along the axial direction is also reduced in direct correlation with the helix angle of the spiralling walls. This is also reflected in the lower Young's modulus values recorded and the greater splitting resistance observed in compression tests.

(c) Filaments drawn through spiralling dies are more dimensionally stable than those produced with straight dies.

(d) The underlying cause for the difference in properties observed in filaments produced with spiralling-wall dies relative to those made with convergent straight-wall dies is the lower level of molecular orientation within the amorphous phase.

References

[1] Ward IM. Plast Rubber Int 1989;14:26.
[2] Perkins WG, Capiati NJ, Porter RS. Polym Engng Sci 1976;16:200.
[3] Brady JM, Thomas EL. Polymer 1989;30:1615.
[4] Zachariades AE, Logan JA. J Appl Polym Sci 1983;28:1837.
[5] Selwood A, Ward IM, Parson B. Plast Rubber Process Appl 1987;8:49.
[6] Mascia L, Zhao J. Adv Polym Technol 1990;10:87.
[7] Mascia L, Zhao J. Rheol Acta 1991;30:369.
[8] Mascia L, Zhao J. Polym Engng Sci 1991;31:369.
[9] Zachariades AE. J Appl Polym Sci 1984;29:867.
[10] Mascia L, Fekkai Z, Guerra G, Parravicini L, Auriemma F. J Mater Sci 1994;29:3151.
[11] Shaw MT. J Appl Polym Sci 1975;19:2811.
[12] Coates PD, Ward IM. J Polym Sci, Polym Phys Ed 1978;16:2031.
[13] Timoshenko SP, Goodier JN. Theory of elasticity, 3rd ed. New York: McGraw-Hill, 1970. p. 308.
[14] Mascia L, Fekkai Z. Polymer 1993;34:1418.
[15] Wilson MPW. Polymer 1974;15:277.
[16] Bhatt GM, Bell JP. J Polym Sci, Polym Phys Ed 1976;14:575.